Dynamics of the globally coupled complex Ginzburg-Landau equation

Vincent Hakim and Wouter-Jan Rappel

*Laboratoire de Physique Statistique, Ecole Normale Supérieure and Universities Paris VI and VII, 24 rue Lhomond,
75231 Paris, CEDEX 05, France*

A discrete version of the complex Ginzburg-Landau equation is studied on a completely connected lattice of N sites. This can equivalently be described as a model of N identical globally coupled limit-cycle oscillators. The phase diagram is obtained by a combination of numerical and analytical techniques. A surprising variety of dynamical behaviors is found in the thermodynamic limit ($N \gg 1$). Depending on the region of parameter space, one gets the following: (1) a simple homogeneous limit cycle; (2) a state with complete frequency locking but with no phase locking so that the global forcing term vanishes; (3) a breaking of the system into a few macroscopic clusters which can exhibit periodic or quasiperiodic dynamics; or (4) surprisingly complex states where an individual oscillator behaves in a chaotic way but in a sufficiently coherent manner so that the average complex amplitude does not vanish in the thermodynamic limit. Moreover, in this last region, the dynamics of this natural order parameter is itself chaotic.

A general understanding of the different dynamical regimes of dissipative systems with many active degrees of freedom is still lacking despite its importance in a wide range of fields. Nevertheless, in recent years, many specific models of spatiotemporal chaos have been the subject of intense investigations [1-10]. In particular, Ginzburg-Landau equations have been used to describe a large range of phenomena [11]. The complex Ginzburg-Landau equation (CGLE) in its simplest version reads as

$$\partial_t A = (1 + i\beta)\nabla^2 A + \mu A - (1 + i\alpha)|A|^2 A . \quad (1)$$

It displays a variety of dynamical regimes in different regions of parameter space. In particular, all plane-wave solutions are unstable for $\alpha\beta + 1 < 0$ [12]. The complicated behavior of the CGLE in this Benjamin-Feir unstable regime has been numerically investigated both in one [9] and in two spatial dimensions [10] and different phases have been numerically characterized. Our aim in this Rapid Communication is to introduce and study a simpler but related model which can be viewed as a mean-field-like version [3,5,8] of Eq. (1). We choose to discretize the CGLE on a fully connected lattice of N sites (i.e., where each point is connected to all the other points). Taking the discrete version of the Laplacian on such a lattice, we obtain, instead of Eq. (1),

$$\partial_t A_j = \frac{1 + i\beta}{N} \sum_{k=1}^{N} (A_k - A_j) + \mu A_j - (1 + i\alpha)|A_j|^2 A_j ,$$
$$j = 1, \ldots, N . \quad (2)$$

This is a system of N identical globally coupled limit-cycle oscillators. Related models of coupled oscillators and coupled maps have already been studied by a number of authors, partially motivated by their connection to such different topics as Josephson-junction arrays [6], oscillatory dynamics of neuronal systems [7,13,14], or synchronized behavior of assemblies of fireflies [8,15]. The present model [Eq. (2)] differs from these previous studies by the

fact that all oscillators are identical (in contrast to [5,8]). Also, they have simple oscillatory dynamics in the absence of interaction (i.e., they cannot exhibit chaotic motion in the absence of coupling like in [3]). Finally, the amplitude dynamical mode is not frozen like in pure-phase models [6,7] and this plays a crucial role in the coherent chaotic dynamical regime that we have found.

Our goal is to determine the asymptotic behavior of (2) in the thermodynamic limit ($N \gg 1$) as a function of the parameters α, β, and μ. We first describe our numerical results. Equation (2) was integrated numerically, using both a fourth-order Runge-Kutta model and an explicit method, with a time step that was generally taken to be $dt = 0.01$ but, if necessary, reduced to $dt = 0.001$ (see below). Lattices of 50 to 5000 sites were used but, in general, reliable results were already obtained with the smaller numbers. Several different initial conditions were tested, such as random initial conditions in a square or circle of variable size.

Four main qualitatively different types of behavior were observed. We restrict ourselves here to the description of the two-parameter space $\alpha = -\beta, \mu$ which appears to be sufficient to describe the qualitatively different phases. They are delimited in Fig. 1 as a function of β and μ. We describe the four different types of behavior in order of increasing complexity.

Region I is the simplest. All the oscillators are in the same state [i.e., $A_j(t) = A(t)$]. Therefore, the coupling term in Eq. (2) vanishes and the oscillators follow the limit cycle of the uncoupled system

$$A(t) = \sqrt{\mu}\exp(-i\alpha\mu t) . \quad (3)$$

This region can be found below and to the left of the line denoted BF (for Benjamin-Feir) in Fig. 1.

Region II is also quite simple. There, all the oscillators are rotating with the same frequency. However, their phases are distributed on the limit circle of radius $\sqrt{\mu - 1}$ in such a way that the forcing mean amplitude $\overline{A}$
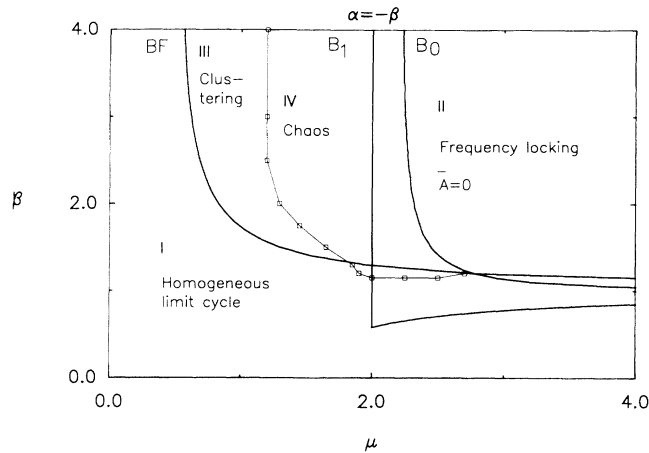
FIG. 1. The phase diagram for the case $\alpha = -\beta$. The line BF is the line at which the homogeneous limit cycle becomes unstable. The line B_0 limits the stability of the solution where all the oscillators are distributed uniformly on a circle of radius $\sqrt{\mu - 1}$. The line B_1 is the limit of stability of the nonuniform locked states. The analytical equations of these lines are given in the main text. The squares are numerically obtained values for the limit of existence of the complex state characteristic of region IV. The thin line is a guide to the eye. For further explanation we refer to the text.

$= (1/N)\sum_j A_j$ vanishes:

$$A_j = \sqrt{\mu - 1} \exp\{i[(\alpha - \beta - \alpha\mu)t + \phi_j]\},$$

$$\text{with } \frac{1}{N}\sum_{j=1}^{N} e^{i\phi_j} = 0. \quad (4)$$

For phases distributed uniformly on the circle (sometimes called "splay-phase" states in the literature [6]), the stability limit is the line B_0 in Fig. 1. However, states distributed unevenly on the limit circle (but still with $\overline{A} = 0$) also exist and have a slightly larger domain of stability. The configuration of this type which has the larger domain of stability is formed by two populations of oscillators, having opposite phases. The boundary of stability of this last configuration is denoted B_1 in Fig. 1. However, in the parameter region between the lines B_0 and B_1, when the oscillator phases were initially distributed uniformly on the limit cycle, we never observed restabilization to a state with an uneven distribution of phases but always a transition towards the chaotic state of region IV described below. In fact, special care was needed in order to observe the stability of the uniform state up to the line B_0 and we found it necessary to reduce the time step to $dt = 0.001$.

In region III, i.e., to the right of the line connecting the open squares and the line BF, the system breaks into a small number N_c of different macroscopic clusters. All the oscillators that belong to a given cluster have the same complex amplitude but it differs from one cluster to the other. Generally, N_c was found to be 2 or 3. Within region III, the dynamics effectively reduces to that of a low number of coupled oscillators (with different weights) and it was found to be periodic or quasiperiodic depending on the parameter subregion.

The behaviors found in regions I, II, and III have already been observed in a number of previous models. In particular, the clustering in region III appears similar to what has been reported for globally coupled logistic or circle maps [3] or homogeneous pure-phase oscillators [7].

In contrast to the first three regions, the behavior in region IV appears surprisingly complex and new. Different oscillators follow different erratic motions but in a sufficiently coherent way so that the mean amplitude, $\overline{A} = (1/N)\sum_j A_j$, remains of order 1 in the thermodynamic limit. Moreover, the dynamics of $\overline{A}$ appears to be chaotic. Although a similar chaotic behavior has been found in [6], we were surprised to observe it with identical oscillators. In order to illustrate and support these assertions different types of numerical evidence are now described. First, in Fig. 2 the position of all the oscillators are shown as dots at two different times, together with the position of the mean (the crosses in Fig. 2). The parameters values are given in the caption. These two times have been chosen to be large enough to be representative of what is observed in the long-time limit, at least with our numerical capabilities. At a given time instant, different oscillators are located at different position in the complex plane, along a shape that has roughly the form of a ρ. The whole shape rotates and also deforms in time, especially in the tail part. Individual oscillators move along this shape, fast motion around the loop of the ρ alternating with slow motion in the tail part. The time evolution of the real part of the mean complex amplitude $\overline{A}(t)$ is represented in Fig. 3(a) together with the power spectrum for this time series [Fig. 3(b)]. The power spectrum is peaked around a definite frequency but appears to be broadband. Moreover, its width does not decrease when the number of oscillators is enlarged from 50 to 5000.

In order to get additional evidence on the chaotic nature of the dynamics the spectrum of Lyapunov exponents for the whole dynamical system has been computed. The number of positive Lyapunov exponents has been found to increase with the number of oscillators. In contrast to this high-dimensional dynamics, we believe that the reduced
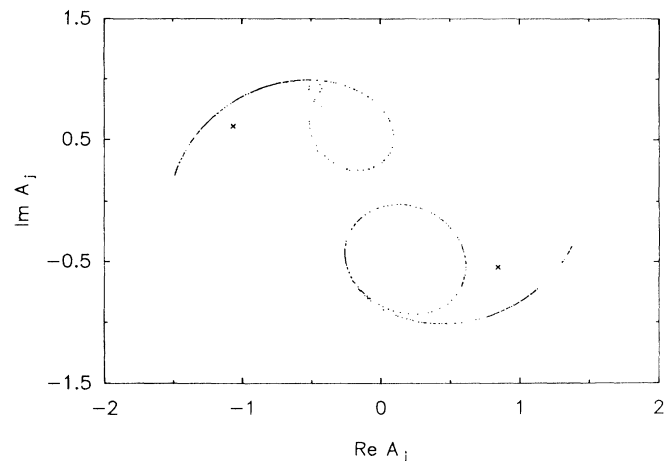

FIG. 2. The positions of the 500 individual oscillators (dots) and their mean (crosses) in the complex plane at two different times. The parameter values are $\mu = 2.0$ and $\beta = 1.5$.
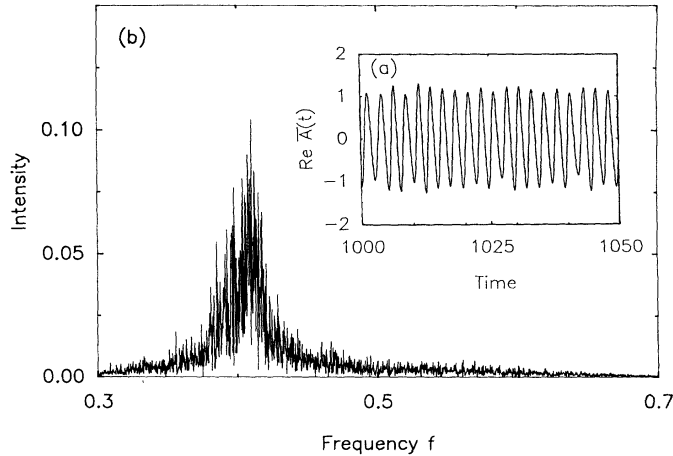
FIG. 3. (a) The time series of the mean for the parameter values of Fig. 2. (b) The power spectrum corresponding to this time series.

dynamics of the average amplitude $\overline{A}(t)$ is low dimensional, in the thermodynamic limit. We have tried to get numerical evidence for that by computing the correlation dimension of the corresponding time series [16,17]. Although our data seems to saturate for embedding dimensions larger than four for not-too-small correlation balls, the scaling window was found to be too small to get a reliable estimate of the correlation dimension. The difficulty seems similar to what would be obtained for the noninteracting product dynamics of a low-dimensional dynamical system and a high-dimensional noise signal of smaller amplitude (see [17] for a discussion).

We now summarize our analytical calculations of the boundaries of the different dynamical regimes. Our calculation of the homogeneous limit-cycle stability (regime I) is very similar to the classical calculation of the Benjamin-Feir instability in the envelope equation framework [12,18]. Equation (2) is linearized into a linear dynamical system of N coupled equations for N complex coefficients a_j by writing $A_j = (\sqrt{\mu} + a_j)\exp(-ia\mu t)$, $|a_j| \ll 1$. The associated real stability matrix of size $2N \times 2N$ is easily diagonalized due to its large symmetry. One obtains one zero eigenvalue coming from the invariance of Eq. (2) under a global phase change, one negative eigenvalue -2μ and $N-1$ sets of two eigenvalues λ_1 and λ_2, solutions of the real second-order equation

$$\lambda^2 + 2(\mu + 1)\lambda + 2\mu(1 + \alpha\beta) + 1 + \beta^2 = 0. \tag{5}$$

The condition of instability of the homogeneous limit cycle, which is that some eigenvalues have a real positive part, is therefore equivalent to the condition $\lambda_1\lambda_2 < 0$ (since the sum $\lambda_1 + \lambda_2$ is negative). In our case, the Benjamin-Feir instability line is thus given by $2\mu(1 + \alpha\beta) + (1 + \beta^2) = 0$. This is the line denoted BF in Fig. 1 for the case $\alpha = -\beta$.

The calculation of the stability of the locked states characteristic of region II is similar but slightly more tedious. Equation (2) is linearized around an arbitrary locked state [Eq. (4)] by writing

$$A_j = (\sqrt{\mu - 1} + a_j)\exp\{-i[\beta + \alpha(\mu - 1)]t + \phi_j\},$$

$$|a_j| \ll 1. \tag{6}$$

The large symmetry of the associated $2N \times 2N$ real stability matrix is again very helpful in diagonalizing it. We find $N-2$ negative eigenvalues equal to $-2(\mu - 1)$ and $N-2$ zero eigenvalues, reflecting the dimensions of the manifold of locked fixed points (i.e., N arbitrary real phases subject to the condition $\overline{A} = 0$ which gives two real constraints [19]). The four remaining eigenvalues depend on the particular locked state under consideration but only through the real parameter $\Delta = |(1/N)\Sigma_j\exp(2i\phi_j)|$, $0 \le \Delta \le 1$, which characterizes the repartition of the oscillator phases on the limit cycle. For $\Delta = 0$ the degree-4 characteristic polynomial $P_4(\lambda)$ whose roots are then searched for eigenvalues, factorizes into two degree-2 polynomials with complex conjugate coefficients $P_2(\lambda)$ and $P_2^*(\lambda)$,

$$P_2(\lambda) = \lambda^2 - \lambda(3 - 2\mu + i\beta) - (\mu - 1)(1 + i\beta)(1 - i\alpha). \tag{7}$$

When a root of Eq. (7) has a positive real part all the states with $\Delta = 0$ are unstable. The corresponding B_0 line is plotted in Fig. 1. When $\Delta \ne 0$ the 4×4 stability matrix no longer splits into two 2×2 matrices and its characteristic polynomial is given by

$$P_4(\lambda) = P_2(\lambda)P_2^*(\lambda) - \Delta^2(\mu - 1)^2(1 + \alpha^2)(1 + \beta^2). \tag{8}$$

For $\alpha = -\beta$ we have checked that the larger Δ, the wider is the stability domain of the corresponding locked states. In this case, $P_4(\lambda)$ also factorizes for the $\Delta = 1$ most stable state which corresponds to a population of oscillators evenly split between two clusters of opposite phases:
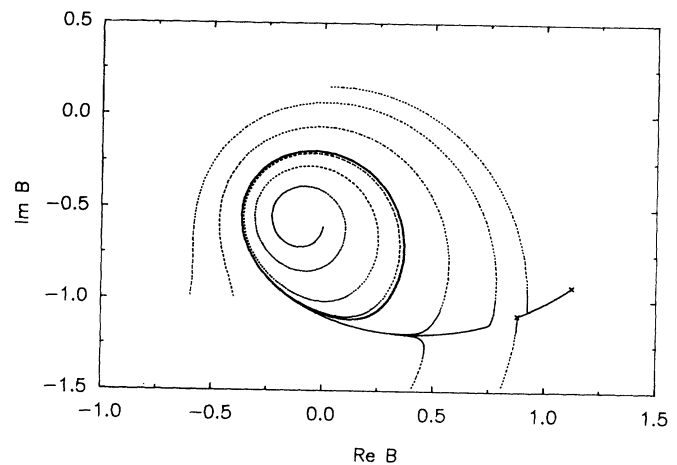

FIG. 4. The phase space of one oscillator driven by a purely periodic force [Eq. (10)] for $\alpha = -1.5$, $\Omega = -4.1$, and $F = 2.11$. Different individual trajectories have been plotted in order to show the existence of an attractive limit cycle and the presence of a couple of fixed points, one stable and one unstable. When the amplitude of the driving force is slightly reduced the two fixed points collide and disappear, leaving only the stable limit cycle.

$$P_4(\lambda) = \lambda[\lambda + 2(\mu - 1)][\lambda^2 + 2(\mu - 2)\lambda + 3$$

$$- \beta^2 + 2\mu(\beta^2 - 1)] . \qquad (9)$$

The domain of stability of the $\Delta = 1$ state is thus the region $\mu \geq 2$, $\beta \geq \sqrt{(2\mu - 3)/(2\mu - 1)}$ whose boundary is denoted by B_1 in Fig. 1.

The complex states characteristic of region IV appear as one of our most intriguing numerical findings. A first simple approach has been followed in order to gain some understanding of the dynamics in this phase. As can be seen in Fig. 3, the dynamics of $\overline{A}(t)$ is strongly peaked around a well-defined frequency ν, $\overline{A}(t) = R(t)$ $\times \exp(i2\pi\nu t)$, where $R(t)$ varies slowly compared to the exponential factor. This suggests to consider the dynamics of a single oscillator $A(t)$ driven by a periodic force of frequency ν and constant amplitude R close to the average amplitude $\langle R(t) \rangle$. This is conveniently done by going to a frame rotating at frequency ν. Defining $A(t) = \sqrt{\mu - 1}$ $\times B(t)\exp(i2\pi\nu t)$ one gets the simple evolution equation for $B(t)$

$$\partial_\tau B = (1 + i\Omega)B - (1 + ia)|B|^2 B + F \qquad (10)$$

with

$$\Omega = -\frac{2\pi\nu + \beta}{\mu - 1}, \quad |F| = \frac{(1 + \beta^2)^{1/2}}{(\mu - 1)^{3/2}} R . \qquad (11)$$

A rescaled time $\tau = (\mu - 1)t$ has also been introduced in order to show explicitly that the dynamics of $B(t)$ in the rotating frame depends only on the two effective parameters Ω and $|F|$. In the parameter range corresponding to the complex chaotic state of region IV the phase space of Eq. (10) seems to be close to a bifurcation between two topologies. For example, simulation of the full system [Eq. (2)] with $\beta = -\alpha = 1.5$ and $\mu = 2$ gives for the main frequency $\nu \simeq 0.41$ and $\langle |\overline{A}(t)| \rangle \simeq 1.1$. The corresponding effective parameters for the reduced system are $\Omega \simeq -4.1$ and $|F| \simeq 2.0$. Fixing Ω to this latter value, the topology of the phase space of Eq. (10) changes for $F_c = 2.08$. As shown in Fig. 4, for $|F| \geq F_c$, there is an attractive limit cycle and a pair of fixed points outside the limit cycle, one stable and one unstable. However, as F decreases toward F_c, these two fixed points move toward each other and they disappear at $|F| = F_c$ in a usual saddle-node bifurcation [20]. For the full system, neither of these two cases appears to be realizable in a stable self-consistent way. It then evolves continuously between the two situations, the operating point remaining close to $|F| = F_c$. This gives rise to the ρ-shaped distribution of oscillators observed in region IV. A precise characterization of this dynamics will hopefully be possible to obtain by refining the present approach to take into account a slow evolution of $R(t)$.

[1] Y. Kuramoto, *Chemical Oscillators, Waves and Turbulence* (Springer, New York, 1984).

[2] H. Chaté and P. Manneville, Prog. Theor. Phys. (to be published).

[3] K. Kaneko, Phys. Rev. Lett. **63**, 219 (1989); **65**, 1391 (1990); Physica D **55**, 368 (1992), and references therein.

[4] Y. Pomeau, Physica D **23**, 3 (1986); H. Chaté and P. Manneville, Europhys. Lett. **6**, 59 (1988); Physica D **32**, 409 (1988); P. Manneville, in *Propagation in Systems Far from Equilibrium*, edited by J. E. Weisfreid *et al.* (Springer, New York, 1988).

[5] Y. Kuramoto and Y. Nishikawa, J. Stat. Phys. **49**, 569 (1987); H. Daido, Phys. Rev. Lett. **68**, 1073 (1992).

[6] K. Wiesenfeld and P. Hadley, Phys. Rev. Lett. **62**, 1335 (1989); J. W. Swift, S. H. Strogatz, and K. Wiesenfeld, Physica D **55**, 239 (1992).

[7] D. Golomb *et al.*, Phys. Rev. A **45**, 3516 (1992).

[8] P. C. Matthews and S. H. Strogatz, Phys. Rev. Lett. **65**, 15 (1990); P. C. Matthews, R. E. Mirallo, and S. H. Strogatz, Physica D **52**, 293 (1991).

[9] B. Shraiman *et al.*, Physica D **57**, 241 (1992).

[10] P. Coullet, L. Gil, and J. Lega, Phys. Rev. Lett. **62**, 1619 (1989).

[11] P. Coullet and G. Iooss, Phys. Rev. Lett. **64**, 866 (1990).

[12] T. B. Benjamin and J. E. Feir, J. Fluid Mech. **27**, 417 (1967); A. C. Newell, Lect. Appl. Math. **15**, 157 (1974); J. T. Stuart and R. C. DiPrima, Proc. R. Soc. London, Ser. A **362**, 27 (1978).

[13] H. Sompolinsky, A. Crisanti, and H. J. Sommers, Phys. Rev. Lett. **61**, 259 (1988).

[14] E. Niebur, H. G. Schuster, and D. M. Kummen, Phys. Rev. Lett. **67**, 2753 (1991).

[15] J. Buck and E. Buck, Sci. Am. **234**, 74 (1976).

[16] P. Grassberger and I. Procaccia, Physica D **9**, 189 (1983).

[17] J. P. Eckmann and D. Ruelle, Rev. Mod. Phys. **57**, 617 (1985), see especially the discussion on p. 648.

[18] Related stability calculations for a chain of coupled oscillators are given in G. B. Ermentrout and N. Kopell, SIAM J. Math. Anal. **15**, 215 (1984). Similar ideas are used for neural-like oscillators by A. Sherman and J. Rinzel, Proc. Natl. Acad. Sci. U.S.A. **89**, 2471 (1992).

[19] $N - 2$ zero eigenvalues are also found when the stability of "splay-phase states" is investigated for a series arrays of N Josephson junctions [S. Nichols and K. Wiesenfeld, Phys. Rev. **45**, 8430 (1992), and references therein]. It would be interesting to see whether this is due to the existence of more general locked states with nonuniform time delays as in the present case.

[20] The critical value F_c is given as a function of the two parameters of the reduced system Ω and α [Eq. (10)] by

$$F_c^2 = [2(1 + \Omega\alpha)^3/27(1 + \alpha^2)^2]$$
$$\times (1 + 9[(\Omega - \alpha)/(1 + \Omega\alpha)]^2$$
$$- \{1 - 3[(\Omega - \alpha)/(1 + \Omega\alpha)]^2\}^{3/2}) .$$